Palomares Gimeno, AE.; Uzcategui Paredes, A.; Franch Martí, C.; Corma Canós, A. (2013). Multifunctional catalyst for maximizing NOx oxidation/storage/reduction: The role of the different active sites. Applied Catalysis B: Environmental. 142-143:795-800. doi:10.1016/j.apcatb.2013.06.015.

Applied Catalysis B: Environmental 142–143 (2013) 795–800

Contents lists available at SciVerse ScienceDirect

Applied Catalysis B: Environmental

journal homepage: www.elsevier.com/locate/apcatb

Multifunctional catalyst for maximizing NO_x oxidation/storage/reduction: The role of the different active sites

E. Palomares*, A. Uzcátegui, C. Franch, A. Corma

Instituto de Tecnología Química, Universidad Politécnica de Valencia-CSIC, Avenida de los Naranjos s/n, 46022 Valencia, Spain

ARTICLE INFO

Article history:
Received 12 April 2013
Received in revised form 13 June 2013
Accepted 17 June 2013
Available online xxx

Keywords:
NO_x
Storage reduction catalysts
Hydrotalcites
Mg/Al/Co mixed oxides
Vanadium
Sodium

ABSTRACT

A multifunctional catalyst/storage material has been prepared to maximize NO_x removal. This material is based on mixed oxides derived from modified layered double hydrotalcites (LDH). A cobalt catalytic function oxidizes the NO to NO_2. The NO_2 is stored as nitrate in the basic sites of the material. The basic properties of the Co/Mg/Al mixed oxide derived from LDH were enhanced by doping with sodium, improving the storage capacity of the catalyst. Finally, the introduction of vanadium sites, enables the reduction–decomposition of the nitrates. This multisite catalyst/storage material results in a well equilibrate formulation that maximizes catalyst conversion and regenerability.

1. Introduction

Hydrotalcites are layered double hydroxides (LDH) with a general formula of $[M_{1-x}^{2+}M_x^{3+}(OH)_2]A_{x/m}^{m-}\cdot zH_2O$. They present positively charged layers brucite-like ($Mg(OH)_2$) with trivalent cations substituting divalent cations in octahedral sites. A wide range of derivatives containing various combinations of M^{2+}, M^{3+} and A^{n-} ions can be synthesized and several reviews have been published reporting their preparation, characterization and applications [1–3]. Hydrotalcites are thermally stable up to 400 °C but they are transformed into mixed metal oxides or spinels at higher temperatures [4]. Calcined hydrotalcites are potentially useful as catalysts or catalyst precursors since they present a high surface area and a basic character. Some examples of the use of Mg–Al hydrotalcites as active and selective catalysts in various base-catalyzed reactions have been reported [5–13]. They have also been used as catalysts or catalyst support in redox reactions by incorporating transition metals with redox properties in their structure [10–17].

The combination of basicity and redox properties is the basis of the NO_x storage–reduction (NSR) catalysts [18–20]. These catalysts store the NO_x as nitrates on lean (oxidizing) conditions and reduce the stored nitrates under the rich (reducing) conditions. NSR catalysts are typically composed of at least one basic compound (alkaline or alkaline-earth oxides) and at least one precious-metal component. One of the most common formulation uses Pt and Ba supported on Al_2O_3 [21]. The problem of this material is its fast poisoning by sulphur compounds, its low activity at low temperatures and, specially, the cost of the precious metal [21–23]. Mixed oxides derived from hydrotalcites have also been proposed as active catalysts in this reaction [24–32]. However, their oxidative activity, storage capacity and regenerability are not well balanced, resulting in relatively low levels of conversion after repeated cycles when compared with the $Pt/BaO–Al_2O_3$ catalysts. In order to solve these problems, Cu, Ca, Co, La, Fe, Ru, Mn, Zr, Pd and Pt [26–36] have been introduced during the synthesis and/or by post-synthesis treatments and the results have improved, but more active catalysts are still necessary.

In this work, we present a trifunctional catalyst derived from hydrotalcites, that uses cobalt for the NO to NO_2 oxidation and that has been doped with sodium to increase its alkalinity and with vanadium to increase its regenerability. The role of the different active sites has been studied by comparing the storage capacity of this material in several lean–rich cycles with that of similar materials but without containing sodium, vanadium or cobalt in its composition.

2. Experimental

2.1. Materials

Co(II)Mg(II)Al(III) hydrotalcites were prepared by a standard co-precipitation procedure using two solutions. The first solution contained $Mg(NO_3)_2\cdot 6H_2O$, $Al(NO_3)_3\cdot 9H_2O$ and $Co(NO_3)_2\cdot 3H_2O$

* Corresponding author. Tel.: +34 96 3877800; fax: +34 96 387780.
E-mail address: apalomar@iqn.upv.es (E. Palomares).

0926-3373/$ – see front matter © 2013 Elsevier B.V. All rights reserved.
http://dx.doi.org/10.1016/j.apcatb.2013.06.015

Table 1
Chemical composition (determined by ICP) and textural characteristics of the calcined samples.

Sample	Co/Mg/Al (molar ratio)	% Na (weight)	% V (weight)	Surface area ($m^2\,g^{-1}$)
Co/Mg/Al	14/70/16	–	–	152
Na–Co/Mg/Al	14/70/16	3.5	–	62
V–Co/Mg/Al	15/69/16	–	0.5	143
Na–V–Co/Mg/Al	15/70/15	3.7	0.4	63
Mg/Al	0/75/25	–		207
Na–Mg/Al	0/75/25	3.6		91
V–Mg/Al	0/75/25	–	0.4	203

with a (Al + Mg + Co) molar concentration of 1.5. The second solution contained NaOH and Na_2CO_3 in the adequate concentration to obtain the total precipitation of aluminium, magnesium and cobalt in the former solution and to fix the pH at a value of 13. Both solutions were added, while vigorously stirring, at a total flow-rate of 20 cc h^{-1} for 5 h. The gel was aged under autogenous pressure conditions at 60 °C for 14 h, then filtered and washed with distilled water until the pH was 7 and carbonates were not detected in the filtrate. Mg(II)Al(III) hydrotalcites were prepared as it is described above but without introducing the cobalt salt. The hydrotalcites were calcined at 550 °C in air for 6 h before reaction, obtaining a mixed oxide. Some samples were impregnated by incipient wetness, with NaOH and/or NH_4VO_3 and calcined at 550 °C for 12 h in order to prepare calcined hydrotalcites doped with vanadium and/or sodium. The chemical composition of the different samples is shown in Table 1.

The BET surface area of the catalysts was obtained in a Micromeritics ASAP 2000 apparatus, using the BET method from the nitrogen adsorption isotherms at 77 K.

X-ray diffraction patterns (XRD) of the catalysts were collected with a PHILLIPS X'Pert-MPD diffractometer provided with a graphite monochromator, operating at 40 kV and 20 mÅ and employing nickel-filtered CuKα radiation (λ = 0.1542 nm).

The chemical composition of the samples was measured by ICP-OES. The samples (*ca.* 20 mg) were dissolved in a HNO_3/HCl (1:3, vol.) solution before analysis in a Varian 715-ES ICP-Optical Emission Spectrometer.

Fourier transform infrared spectra were recorded in transmission mode, with potassium bromide pressed disks, by accumulating 32 scans at 4 cm^{-1} resolution between 400 and 4000 cm^{-1} using a Nicolet 710 Fourier Transform Infrared spectrometer.

A Fissons EA-1108CHNS-O elemental analyzer was used in order to determine the N content of the samples.

2.2. Catalytic experiments

The reaction experiments were carried out in a fixed bed, tubular reactor (2.2 cm diameter and 53 cm length). In the experiments 1 g of catalyst, as particles of 0.25–0.42 mm, was introduced in the reactor and was heated up to 450 °C under nitrogen flow. At this temperature the flow was maintained for 2 h. After that, the desired reaction temperature was set and 650 ml min^{-1} of a mixture composed by NO, C_3H_8, oxygen and balanced with nitrogen, was admitted. Catalytic tests were performed at different temperatures (450, 300 and 150 °C) using a cyclic sequence of changes in the feed composition, simulating [37] car exhaust emissions in lean (120 s: 8% O_2, 300 ppm NO_x, 900 ppm C_3H_8, N_2 balance) and rich conditions (60 s: 0% O_2, 300 ppm NO_x, 900 ppm C_3H_8, N_2 balance). After evaluating the catalyst behaviour during a sequence of 10 lean–rich cycles at a given temperature (450, 300 or 150 °C), the reactor temperature was changed and the catalytic activity was further monitored over ten lean–rich cycles. At the end of the experiments the catalyst was tested again at the initial temperature (450 °C) in order to check the deactivation of the catalyst during the previous experiments. The NO_x present in the gas were analyzed continuously by means of a Thermo 62C chemiluminescence detector.

The thermal stability of the material has been tested by steaming the catalyst with water at 700 °C during 5 h in an oven and by studying its catalytic performance after this treatment.

3. Results and discussion

The chemical composition and surface areas of the catalysts are comparatively shown in Table 1. The catalysts containing cobalt have a Co/Mg/Al molar ratio close to 15/70/15 while the catalysts without cobalt have a Mg/Al molar ratio of 75/25. Some catalysts were impregnated with a solution containing sodium and/or vanadium in order to dope some samples with 3.5% wt sodium and 0.5% wt vanadium. As it can be seen in Table 1, the parent materials present a high surface area between 150 and 210 $m^2\,g^{-1}$ corresponding the highest surface area to the catalyst without cobalt. The addition of vanadium results in a moderate decrease of the surface area, while addition of sodium results in an important decrease of the catalyst surface area that, as indicated by XRD, is probably related with a phase segregation in the parent material.

As can be seen in Fig. 1, the X-ray diffractogram of the calcined Mg/Al/Co hydrotalcites (Fig. 1A) shows the formation of a poorly crystalline cubic magnesium oxide with peaks at 2θ = 36.9, 42.9 and 62.3°. These peaks are shifted to higher angles if compared with a pure magnesium oxide, probably as a consequence of the incorporation of aluminium and cobalt in the framework of the MgO, resulting in the formation of a mixed oxide [38]. No peaks assigned to cobalt species are observed, indicating a good dispersion of the cobalt in the matrix. The impregnation of the sample with a vanadium salt, followed by calcination, does not result in significant changes with respect to the starting material and formation of new

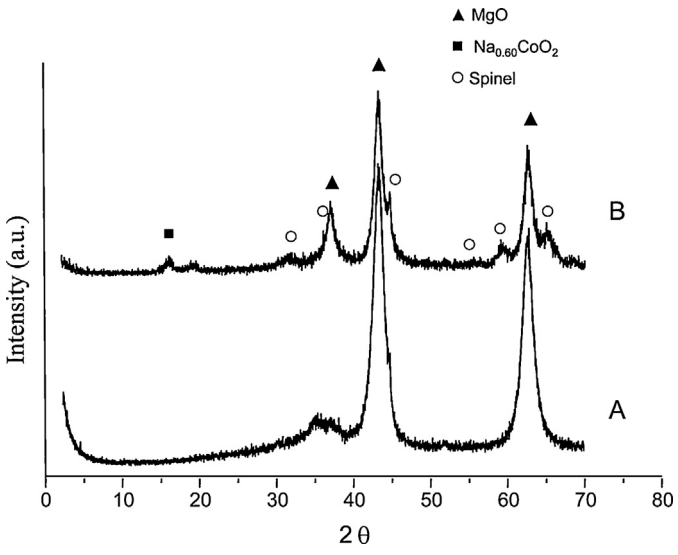

Fig. 1. X-ray diffraction patterns of the calcined Co/Mg/Al hydrotalcite (A) and calcined Co/Mg/Al hydrotalcite doped with sodium (B).

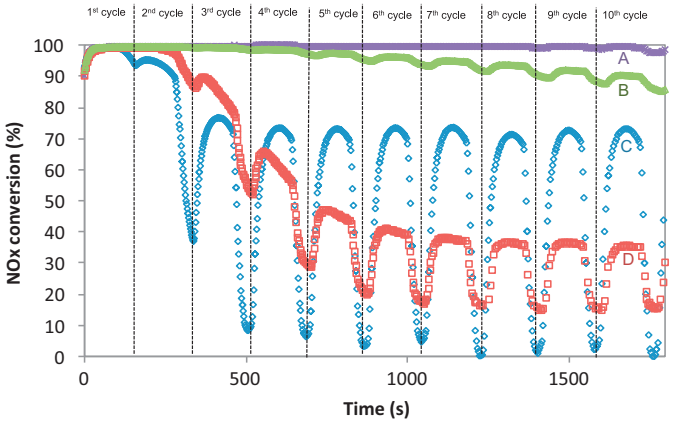

Fig. 2. Dynamic evolution for the NO_x conversion during successive lean–rich cycles with the Co/Mg/Al catalyst doped with sodium and vanadium at 450 °C (A) and 300 °C (B), and with the non-doped Co/Mg/Al catalyst at 450 °C (C) and 300 °C (D).

phases were not detected by XRD. This indicates that the crystallite size of the cubic mixed oxides is the same and that there is a good dispersion of the metal on the catalyst surface. On the other hand, significant differences in the X-ray diffractograms were observed in the Co/Mg/Al catalysts containing sodium (Fig. 1B). In these samples together with the peaks assigned to the MgO, some peaks at $2\theta = 31$, 36, 45, 55, 59 and 65° are observed in the X-ray diffractogram that can be related to $MgAl_2O_4$, $CoAl_2O_4$, Co_2AlO_4 and/or Co_3O_4 spinels. In addition, a small weak peak at $2\theta = 15°$ is observed that only appears in the catalysts derived from Co/Mg/Al hydrotalcites containing sodium and which could be assigned to the (0 0 3) peak of a $Na_{0.60}CoO_2$ phase [39]. This phase [40] exhibits a lamellar structure, and it is based on stacked CoO_2 slabs. Cobalt in this phase has an average oxidation state of 3.4 and the phase exhibits metallic properties [41]. The segregation and formation of these new phases are probably the reason for the decrease of the catalyst surface area (Table 1).

Co/Mg/Al calcined hydrotalcite has been previously described as an active NSR catalyst but its activity was only moderate [24]. However, one can see in Fig. 2 that the NO_x conversion dramatically increases when the catalyst is doped with sodium and vanadium. At 450 °C the non-doped catalyst only removes completely the NO during two lean periods, falling down the conversion during the second rich period without recovering the initial values in the successive cycles (with a rate of 1.015×10^{-7} mol s^{-1} g^{-1} in the steady state). At 300 °C, the decrease in the activity of the Co/Mg/Al catalyst after the first cycle is even more intense. On the contrary, the catalyst containing vanadium and sodium shows no deactivation at 450 °C, removing completely the NO_x both in the rich and in the lean cycles (with a rate of at least 1.450×10^{-7} mol s^{-1} g^{-1}). At 300 °C, there is a small decrease of the NO_x conversion, but a conversion of 85% is still obtained after the ten lean–rich cycles. From these results we thought that a Co/Mg/Al calcined hydrotalcite doped with sodium and vanadium could be worth to investigate as a noble metal free NSR catalyst with well balanced redox and acid–base properties.

In order to understand the role of the different active sites in the reaction, different Co/Mg/Al catalysts containing only sodium or vanadium were prepared and the catalytic results obtained with these materials were compared with those of the Co/Mg/Al catalyst containing both vanadium and sodium. The catalytic tests were performed in a sequence of 10 lean–rich cycles made successively at 450 °C, 300 °C, 150 °C and again at 450 °C. The last experiment is necessary in order to determine the stability of the catalyst and its deactivation during the successive lean/rich cycles at different temperatures. In Fig. 3 we have plotted the mean conversion of the different samples after 10 lean–rich cycles at 450 °C (in the first experiment made at this temperature) and the mean conversion obtained in the experiment made again at 450 °C, but after 30 successive lean–rich cycles at different temperatures. As it can be seen there, all catalysts containing sodium show initially the highest conversion, obtaining a 100% conversion with the Co/Mg/Al catalyst containing only sodium. Unfortunately, this catalyst deactivates during the successive reactions at lower temperatures and the initial activity is not recovered. On the other hand catalysts containing vanadium show almost no deactivation in the successive reaction cycles. In fact, as it can also be seen in Fig. 4, where the dynamic evolution of the NO_x conversion is presented, the Co/Mg/Al calcined hydrotalcite containing vanadium, but no sodium, shows no deactivation at all after 30 lean–rich cycles at different temperatures.

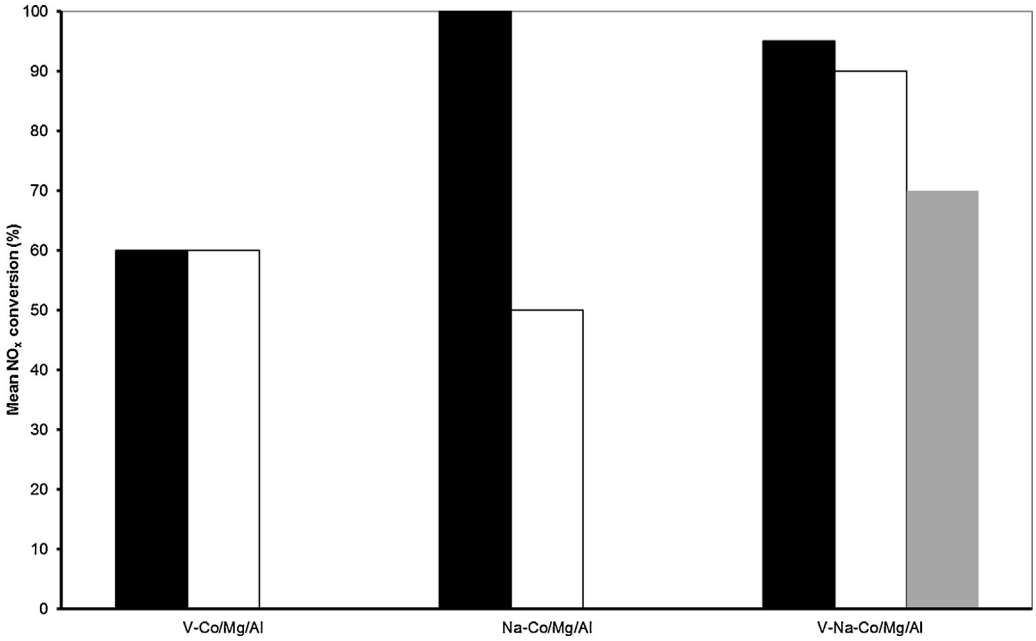

Fig. 3. Mean NO_x conversion (over ten lean–rich cycles) at 450 °C (■), mean NO_x conversion (over ten lean–rich cycles) at 450 °C after 30 successive lean–rich cycles at different temperatures (□) and mean NO_x conversion (over ten lean–rich cycles) at 450 °C in presence of 60 ppm of SO_2 and 8% of water (■) on doped Co/Mg/Al catalysts.

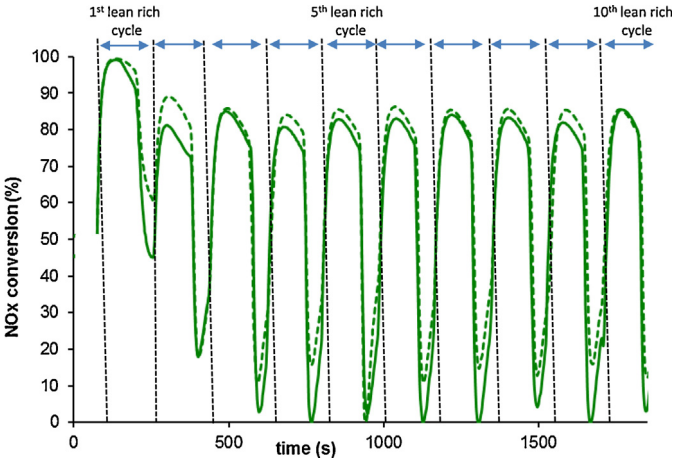

Fig. 4. Dynamic evolution of the NO_x conversion with the Co/Mg/Al catalyst doped with vanadium during the initial ten cycles lean–rich (120 s lean–60 s rich) at 450 °C (–) and during the last ten cycles lean–rich made at 450 °C (----) but after 30 successive lean–rich cycles at different temperatures.

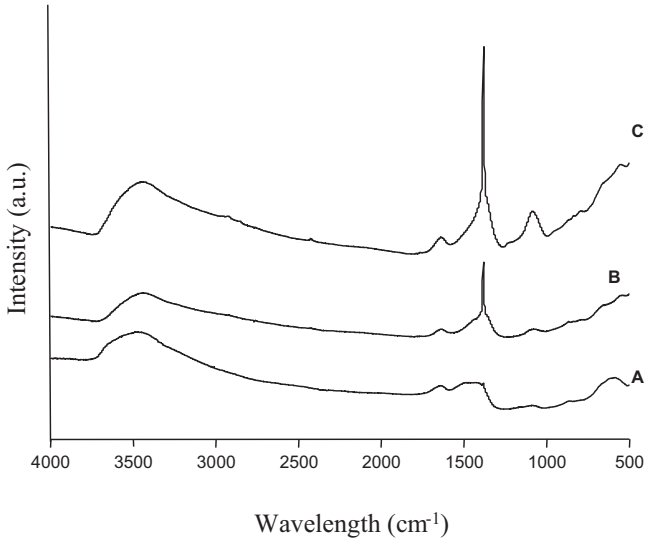

Fig. 5. Infrared spectra, after reaction, of the Co/Mg/Al catalysts doped with vanadium (A), sodium and vanadium (B) and sodium (C).

Nevertheless, this catalyst has a low NO_x storage capacity, especially at low temperatures. In other words, it seems from the above results that the presence of sodium would increase the NO_x storage capacity, while vanadium would favour the regeneration of the catalyst. As we have shown, the introduction of both sodium and vanadium as additional functions into the Co/Mg/Al starting catalyst represents a good compromise between conversion and regeneration in the successive lean–rich cycles.

Comparing the activity if this catalysis with that of a standard $Pt/BaO/Al_2O_3$ [32], it was observed that the mean conversion obtained with the Na/V–Co/Mg/Al catalyst (95% at 450 °C) is better than that obtained with the Pt–Ba catalyst (70% at 400 °C and 55% at 500 °C) or with a catalyst based in Mg/Al hydrotalcites containing Pt (80% at 400 °C and 55% at 500 °C) [32]. Both catalysts show a similar stability in extended catalytic tests (made during 5 h), being the main advantage of the Na/V–Co/Mg/Al catalyst the absence of noble metals in its composition. This results in a lower price for this catalyst although some concerns should be addressed because the highest toxicity of these metals compared with those used in a standard Pt–Ba catalyst.

The hydrothermal stability of the catalyst containing sodium and vanadium and its catalytic performance in presence of SO_2 and water was studied. It was found that after a hydrothermal treatment of the catalyst at 700 °C the same catalytic results at 450 °C were obtained with the aged sample than with the original sample. Similar results were shown by Centi et al. when using a Mg/Al hydrotalcite containing both Pt and Cu [32], obtaining better results than those obtained with a hydrothermally treated standard $Pt/BaO/Al_2O_3$ catalyst. These results confirm the high hydrothermal stability of this type of materials. On the other hand, in presence of water and SO_2, the mean conversion of the catalyst decreases from 95% to 70% (Fig. 3). As it was observed by infrared spectroscopy, this is probably due to the formation of $MgSO_4$ and $NaSO_4$ under lean conditions. Although the decomposition of these sulphates can be catalyzed by the vanadium present in the catalyst under reducing atmosphere, the reaction is relatively slow at temperatures below 500 °C [10] resulting in a partial deactivation of the catalyst.

The catalytic results together with infrared and XRD characterization of the catalysts give some information on the role of the different active sites. These results indicate that the sodium sites are only related with the storage capacity of the catalyst during the lean cycles, while the vanadium sites are related with the regeneration capacity of the catalyst during the rich cycles. In this way the addition of sodium increases the alkalinity of the system resulting in a higher storage capacity of the NO_x as nitrates. This is consequence of the lower electronegativity of sodium with respect to magnesium that results in an increase of the base strength of the lattice, leading to a stronger bonding between the NO_x and the oxides. The infrared study of the different catalysts after reaction (Fig. 5) could support this hypothesis. As the reaction finish with a rich cycle, only in the infrared spectrum of the samples with higher storage capacity and lower regenerability a peak assigned to nitrate should be expected. In fact, the samples containing sodium show a sharp and intense band around 1384 cm^{-1} assigned to monodentate nitrate (NO_2 symmetric vibration) and a smaller and broad band at 1080 cm^{-1} assigned to the NO_3 symmetric vibration of the monodentate nitrate [33]. Together with these bands, a broad band at 1490 cm^{-1} assigned to carbonates and two broad bands around 1640 cm^{-1} and 3600 cm^{-1} assigned to water are observed. Although there are not bands assigned to nitrites, we cannot exclude that the NO_x storage proceeds in these catalysts through the "nitrite route" [42], because as it was shown by Ghiotti et al. with other type of hydrotalcites [42], at higher contact times and at higher temperatures the bands related to nitrites disappear as the bands related to nitrates develop. As the infrared spectra were made *ex situ* after reaction, it is quite likely that the nitrites formed at the beginning of the reaction evolve to nitrates that are the final species. The bands assigned to monodentate nitrate are only observed in catalysts containing sodium, which are the catalysts with a higher NO_x initial adsorption capacity. On the contrary, the bands assigned to the monodentate nitrate are not observed in the Co/Mg/Al catalyst containing only vanadium that presents the lowest adsorption capacity and the highest regenerability.

These results are also supported by the XRD characterization of the samples after reaction. As it can be seen in Fig. 6, together with the main peaks at $2\theta = 36.9$, 42.9 and 62.3° assigned to MgO and to the small peaks assigned to an incipient spinel observed before the reaction (Fig. 1B), new peaks at $2\theta = 29.3$, 31, 35.4, 38.9, 48, 56.6 and 59.9° assigned to $NaNO_3$ appear in the samples containing sodium. This shows that the monodentate nitrates observed by infrared spectroscopy are mainly related with the sodium sites. It should be pointed out that together with the formation of these peaks, the peak at $2\theta = 15°$ initially assigned to the $Na_{0.60}CoO_2$ phase disappears indicating that the cobalt is redispersed in the mixed oxide structure while the sodium is reacting with the NO_x in order to form sodium nitrates. On the other hand, the XRD of the Co/Mg/Al

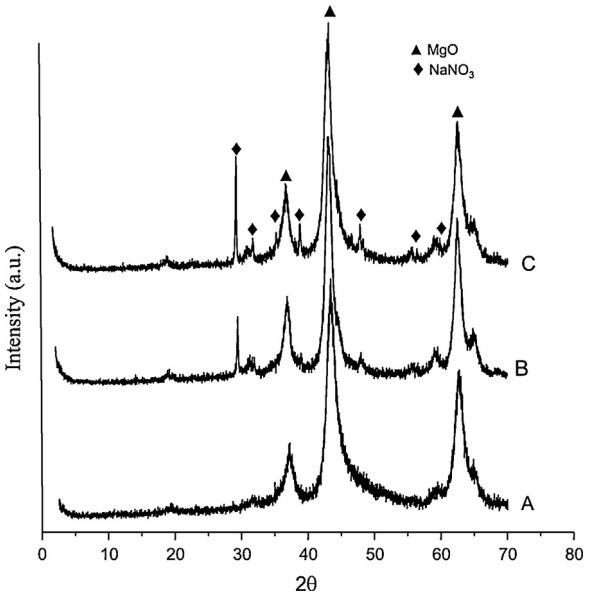

Fig. 6. X-ray diffraction patterns, after reaction, of the Co/Mg/Al catalysts doped with vanadium (A), sodium and vanadium (B) and sodium (C).

catalyst containing vanadium but no sodium shows the peaks assigned to MgO, but no peaks assigned to nitrates are observed. These results clearly confirm the positive role of the Na sites in the NO_x adsorption capacity of the catalyst, but unfortunately the Co/Mg/Al catalyst containing sodium but no vanadium suffers an important deactivation. On the contrary, when vanadium is added to the catalyst, the catalyst is stable after successive lean–rich cycles. This suggests that the presence of vanadium in the catalyst avoid its deactivation, probably because the redox properties of the metal contribute, during the rich cycle, to reduce and to decompose the stored nitrates.

The results presented above show the role for the NSR reaction of sodium and vanadium sites in the doped Co/Mg/Al catalyst, but they do not clarify which is the role of the cobalt sites. To study that, we have prepared a calcined Mg/Al hydrotalcite without cobalt that has been doped with the same content of vanadium or sodium than the Co/Mg/Al catalysts described before. In Fig. 7 the catalytic results obtained with these materials in the NSR reaction have been compared with those of the catalysts containing cobalt. As it can be seen the activity of the former materials is much lower than that of the catalysts containing cobalt. In this case, the presence of sodium in the catalyst also improves the storage of the nitrates and the presence of vanadium also avoids the catalyst deactivation but the results obtained are worse than those obtained with the catalysts containing cobalt. As the only difference in both samples is the presence of cobalt, we can conclude that the role of the cobalt sites is to oxidize the NO to NO_2 in the first part of the reaction. The NO_2 formed will be quickly adsorbed on the basic sites of the catalyst to form nitrites and nitrates [31] on the catalyst surface, leading to a higher activity of the Co/Mg/Al catalysts if compared with the Mg/Al catalysts.

Table 2
N-content (%) in the catalysts after reaction.

Sample	% N (weight)
Co/Mg/Al	0.05
Na–Co/Mg/Al	1.45
V–Co/Mg/Al	0.03
Na–V–Co/Mg/Al	1.15
Na–Mg/Al	0.37
V–Mg/Al	0.06

The N-elemental analysis of the samples after reaction corroborates the results above described. As it can be seen in Table 2, the Mg/Al/Co and the Mg/Al catalysts containing sodium have a higher percentage of the N-compounds than those containing only vanadium that do not present almost any N-compound after reaction. Also it is observed that the Co/Mg/Al catalyst containing sodium has a higher N content than the Mg/Al catalyst containing Na. This is coherent with the results obtained in the catalytic tests and with the XRD and infrared study of the samples, showing the importance of the cobalt for the NO oxidation to NO_2, the role of the sodium sites for the storage of the NO_x in the lean cycles and the

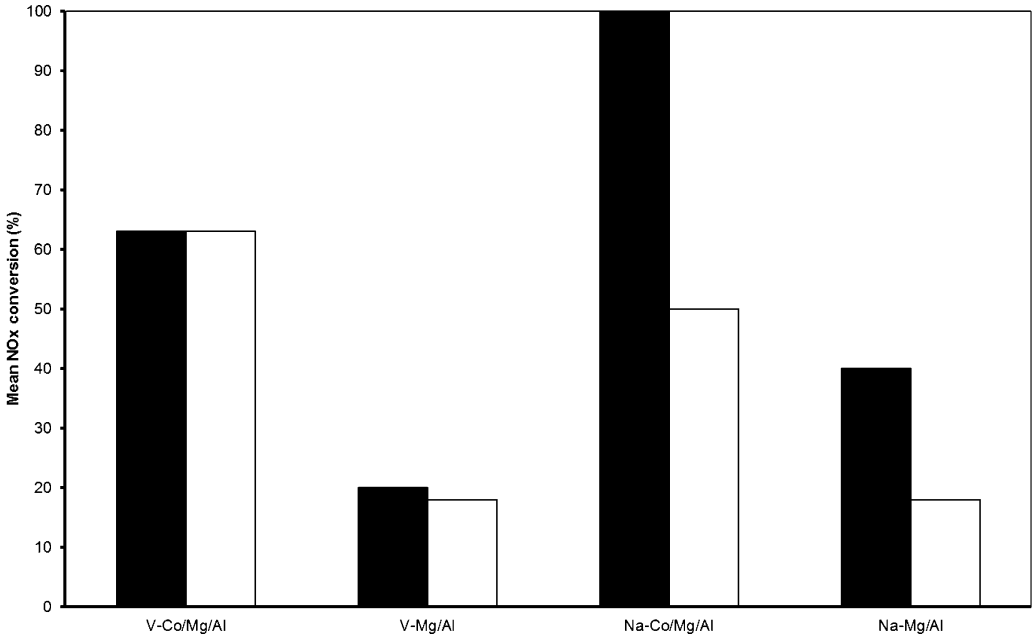

Fig. 7. Mean NO_x conversion (over ten lean–rich cycles) at 450 °C (■) and mean NO_x conversion (over ten lean–rich cycles) at 450 °C after 30 successive lean–rich cycles at different temperatures (□) on Co/Mg/Al and Mg/Al catalysts doped with sodium or vanadium.

importance of the vanadium sites for the regeneration of the catalysts in the rich cycles.

4. Conclusions

From the results obtained in this work, we can conclude that calcined Co/Mg/Al hydrotalcites doped with sodium and vanadium are active NSR catalysts. The presence of cobalt in this catalyst is necessary for the oxidation of the NO to NO_2 that will be adsorbed as nitrate on the catalyst. The presence of vanadium improves the reducibility of the stored nitrates and avoids the deactivation of the catalyst. The presence of sodium increases the basicity of the material improving the nitrate storage capacity. The catalytic tests and the characterization of the samples by XRD, infrared spectroscopy and N-elemental analysis show that when cobalt is present, the NO_x are strongly adsorbed in the sodium sites as monodentate nitrates, being necessary the presence of another transition metal with redox properties as vanadium to decompose/reduce the nitrates during the rich cycle, regenerating the catalyst. An adequate tuning of both basicity and redox properties is necessary in order to find an active NSR catalyst.

Acknowledgements

Financial support from the Spanish Ministry of Economy and Competitiveness through the Severo Ochoa program (SEV-2012-0267) as well as operating grants Consolider Ingenio Multicat (CSD-2009-00050) and MAT-2012-3856-C02-01 is gratefully acknowledged. Authors want to thank Maria Orti for her collaboration in the experiments.

References

[1] P.S. Braterman, P.Z. Xu, F. Yarberri, in: S.M. Auerbach, K.A. Carrado, P.K. Dutta (Eds.), Handbook of Layered Materials, Marcel Dekker, New York, 2004, pp. pp.373.
[2] F. Cavani, F. Trifiró, A. Vaccari, Catal. Today 11 (1991) 173.
[3] M.J. Climent, A. Corma, S. Iborra, K. Epping, A. Velty, J. Catal. 225 (2009) 316.
[4] G.J. Ross, H. Kodarma, Am. Miner. 52 (1967) 1037.
[5] M.J. Climent, A. Corma, S. Iborra, K. Epping, A. Velty, J. Catal. 221 (2) (2004) 474.
[6] A. Guida, M.H. Lhouty, D. Tichit, F. Figueras, P. Geneste, Appl. Catal. A 164 (1997) 251.
[7] S. Velu, C.S. Swamy, Appl. Catal. A 145 (1996) 225.
[8] C. Cativiela, F. Figueras, J.I. Garcia, Synth. Commun. 25 (1995) 1745.
[9] C. Cativiela, F. Figueras, J.M. Fraile, J.I. Garcia, J.A. Mayoral, Tetrahedron Lett. 36 (1995) 4125.
[10] A. Corma, A.E. Palomares, F. Rey, Appl. Catal. B 4 (1994) 29.
[11] A. Corma, A.E. Palomares, F. Rey, F. Marquez, J. Catal. 170 (1997) 140.
[12] F. Márquez, A.E. Palomares, F. Rey, A. Corma, J. Mater. Chem. 11 (6) (2001) 1675.
[13] G. Centi, S. Peratoner, Microporous Mesoporous Mater. 107 (1–2) (2008) 3.
[14] J.M. López Nieto, A. Dejoz, M.I. Vázquez, Appl. Catal. A 132 (1995) 41.
[15] A.E. Palomares, J.G. Prato, F. Rey, A. Corma, J. Catal. 221 (2004) 62.
[16] L. Chmielarz, P. Kustrowski, A. Rafalska-Lasocha, D. Majda, R. Dziembaj, Appl. Catal. B 35 (2002) 195.
[17] Z. Wang, Z. Jiang, W. Shangguan, Catal. Commun. 8 (2007) 1659.
[18] K. Katoh, T. Kihara, T. Asanuma, M. Gotoh, N. Shibaki, Toyota Technol. Rev. 44 (1995) 27.
[19] S. Matsumoto, Y. Ikeda, H. Suzuki, M. Ogai, N. Miyoshi, Appl. Catal. B: Environ. 25 (2000) 115.
[20] E. Friedell, M. Skoglundth, B. Weterberg, S. Johansson, J. Catal. 183 (1999) 196.
[21] W.S. Epling, L.E. Campbell, A. Yezerets, N.W. Curier, J.E. Parks, Catal. Rev. 46 (2) (2004) 163.
[22] L. Limousy, H. Mahzoul, J.F. Brilhac, F. Garin, G. Maire, P. Gilot, Appl. Catal. B: Environ. 45 (2003) 169.
[23] R. Burch, J.P. Breen, F.C. Meunier, Appl. Catal. B: Environ. 39 (2002) 283.
[24] A.E. Palomares, A. Uzcategui, A. Corma, Catal. Today 137 (2008) 261.
[25] F. Basile, G. Fornasari, M. Livi, F. Tinti, F. Trifiro, A. Vaccari, Topics Catal. 30/31 (2004) 223.
[26] G. Fornasari, R. Glockler, M. Livi, A. Vaccari, Appl. Clay Sci. 29 (2005) 258.
[27] B.A. Silletti, R.T. Adams, S.M. Sigmon, A. Nikolopoulos, J.J. Spivey, H.H. Lamb, Catal. Today 114 (2006) 64.
[28] G. Fornasari, F. Trifiro, A. Vaccari, F. Prinetto, G. Ghiotti, G. Centi, Catal. Today 75 (2002) 421.
[29] G. Centi, G. Fornasari, C. Gobbi, M. Livi, F. Trifiro, A. Vaccari, Catal. Today 73 (2002) 287.
[30] J.J. Yu, Z. Jiang, L. Zhu, Z. Ping Hao, Z. Ping Xu, Environ. Sci. Technol. 41 (2007) 1399.
[31] J.J. Yu, J. Cheng, C.Y. Ma, H.L. Wang, L.D. Li, Z.P. Hao, Z.P. Xu, J. Colloid Interface Sci. 333 (2009) 423.
[32] G. Centi, G.E. Arena, S. Perathoner, J. Catal. 216 (2003) 443.
[33] J.J. Yu, Z. Jiang, L. Zhu, Z. Ping Hao, Z. Ping Xu, J. Phys. Chem. B 110 (2006) 4291.
[34] J.J. Yu, X.P. Wang, Y.X. Tao, Z. Ping Hao, Ind. Eng. Chem. Res. 46 (2007) 5794.
[35] J.J. Yu, X.P. Wang, L.D. Li, L. Zhu, Z. Ping Hao, Z. Ping Xu, G.Q. Lu, Adv. Funct. Mater. 17 (2007) 3598.
[36] L.D. Li, J.J. Yu, Z. Ping Hao, Z. Ping Xu, G.Q. Lu, J. Phys. Chem. C 111 (28) (2007) 10552.
[37] J. Dawody, M. Skoglundh, S. Wall, E. Fridell, J. Mol. Catal. A: Chem. 225 (2) (2005) 259.
[38] T. Sato, H. Fujito, T. Endo, M. Shimada, React. Solids 5 (1998) 219.
[39] F. Tronel, L. Guerlou-Demourgues, M. Basterreix, C. Delmas, J. Power Sources 158 (2006) 722.
[40] C. Fouassier, G. Matejka, J.M. Renau, P. Hagenmuller, J.Solid State Chem. 6 (1973) 532.
[41] C. Fouassier, G. Matejka, P. Hagenmuller, Mater. Res. Bull. 10 (1975) 443.
[42] S. Morandi, F. Prinetto, G. Ghiotti, M. Livi, A. Vaccari, Microporous Mesoporous Mater. 107 (2008) 31.